

Accepted Manuscript

Catalytic and stoichiometric oxidation of *N,N*-dimethylanilines mediated by nonheme oxoiron(IV) complex with tetrapyridyl ligand

Dóra Lakk-Bogáth, Balázs Kripli, Bashdar I. Meena, Gábor Speier, József Kaizer

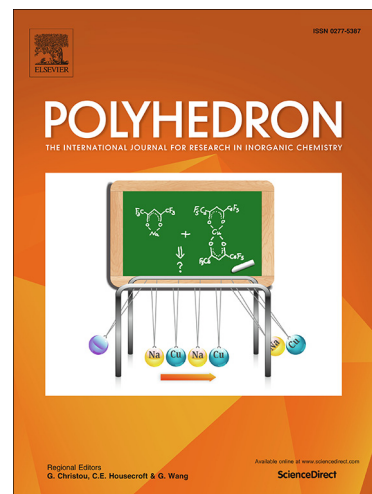
PII: S0277-5387(19)30355-9
DOI: <https://doi.org/10.1016/j.poly.2019.05.025>
Reference: POLY 13950

To appear in: *Polyhedron*

Received Date: 12 April 2019
Accepted Date: 12 May 2019

Please cite this article as: D. Lakk-Bogáth, B. Kripli, B.I. Meena, G. Speier, J. Kaizer, Catalytic and stoichiometric oxidation of *N,N*-dimethylanilines mediated by nonheme oxoiron(IV) complex with tetrapyridyl ligand, *Polyhedron* (2019), doi: <https://doi.org/10.1016/j.poly.2019.05.025>

This is a PDF file of an unedited manuscript that has been accepted for publication. As a service to our customers we are providing this early version of the manuscript. The manuscript will undergo copyediting, typesetting, and review of the resulting proof before it is published in its final form. Please note that during the production process errors may be discovered which could affect the content, and all legal disclaimers that apply to the journal pertain.



Catalytic and stoichiometric oxidation of *N,N*-dimethylanilines mediated by nonheme oxoiron(IV) complex with tetrapyridyl ligand

Dóra Lakk-Bogáth, Balázs Kripli, Bashdar I. Meena, Gábor Speier and József Kaizer*

^aDepartment of Chemistry, University of Pannonia, 8201 Veszprém, Hungary

Abstract

Nonheme iron(II) complex, $[(N4Py^*)Fe^{II}(CH_3CN)](ClO_4)_2$ (**1**) with pentadentate tetrapyridyl ligand ($N4Py^* = N,N$ -bis(2-pyridylmethyl)-1,2-di(2-pyridyl)ethylamine) has been shown to catalyze the oxidation of *N,N*-dimethylaniline (DMA) with H_2O_2 , *tert*-butyl hydroperoxide (TBHP), peracetic acid (PAA), *meta*-chloroperoxybenzoic acid (mCPBA) and PhIO resulting *N*-methylaniline (MA) as the predominant product with *N*-methylformanilide (MFA) as a result of a free-radical chain process. The product composition (MA/MFA) is remarkably influenced by the electron density on the substrate, especially in the **1**/mCPBA system, and by the co-oxidants used. No formation of MFA occurred when the oxidation of DMA was carried out in the presence of **1** with PhIO as co-oxidants under argon.

Based on spectral investigation (UV/Vis) of reaction systems above, oxoiron(IV) intermediate, $[Fe^{IV}(N4Py^*)(O)]^{2+}$ (**2**) has been suggested to be the key active species of the *N*-dealkylation reaction in all catalytic systems. The shift in the λ_{max} value of the oxoiron(IV) species in the presence of DMA from 705 to 750 nm, and the new intense absorption in the range of 5-600 nm indicates a complexation and charge-transfer (CT) type interactions between the oxidant and substrate. The stoichiometric oxidation of various *N,N*-dimethylaniline derivatives with **2** provided clear evidence (Hammett correlation with $\rho = -1.99$, and the large negative slope (-4.1) from the $\log k_{obs}$ versus E^o_{ox} (DMAs) plot) for the rate-determining electron transfer (ET) followed by a proton transfer (PT) process.

Keywords: Bioinspired oxidation, C-H activation, Oxidative *N*-dealkylation, Nonheme oxoiron complex, Kinetics.

*Corresponding author. Tel.: +36 88 62 4720; Fax: + 36 88 62 4469.
E-mail address: kaizer@almos.uni-pannon.hu.

1. Introduction

Heme and non-heme iron-dependent *N*-dealkylation reactions play important roles in numerous biological processes from DNA repair to the metabolism and detoxification of various xenobiotics such as tertiary amine containing drugs [1-7]. For example, 1-methyl-4-phenyl-1,2,3,6-tetrahydropyridine (MPTP) is a neurotoxic byproduct of the heroin synthesis, which is able to induce a Parkinson's disease in humans. Its detoxification by P450s can protect neurons within the central nervous system in humans and in animals [8]. The mechanism of these important processes has been extensively studied but it is still obscured, whether the oxoiron-mediated *N*-dealkylations proceed through a C α -H abstraction and/or a single-electron transfer (SET) mechanism [9-16]. In case of horseradish peroxidase (HRP) the formation of aminium radicals (EPR, electron paramagnetic resonance spectroscopy) during the oxidation process can be explained by the involvement of the rate-determining electron-transfer before the α -hydroxylation step [17,18]. However, direct hydrogen atom transfer (HAT) has been proposed for cytochrome P450 [15,16,19]. 2-Oxoglutarate/Fe(II)-dependent dioxygenases are also known to catalyze *O*- and *N*-demethylation reactions [20]. For example AlkB-type proteins catalyze the removal of *N*-linked methyl groups at positions 1 and 3 of purine and pyrimidine bases, respectively, in DNA and RNA [21]. As a functional models for the iron-containing proteins several catalytic systems have been examined for *N,N*-dimethylaniline (DMA) derivatives. Iron(III)-salen, iron(II, III)-2,2'-bipyridine and iron(III)-porphyrin complexes, furthermore simple iron salts FeCl₃ and Fe(ClO₄)₃ have been developed as catalysts for the oxidation of DMAs with various oxygen sources including iodosobenzene, hydroperoxides and molecular oxygen, resulting a mixture of *N*-methylformanilide (MFA), *N*-methylaniline (MA) and other dimerized products, where the product composition and the mechanism were remarkably influenced by the nature of the iron catalyst used, although the active species in each case is unclear [22-26]. It is worth to mention that *N*-methylformanilide is an important intermediate in organic synthesis, it is widely used in the Vilsmeier reaction [27,28]. Recent reports postulate electron transfer–proton transfer (ET–PT) mechanism for *N*-demethylation of *N,N*-dimethylanilines promoted by [(N4Py)Fe^{IV}(O)]²⁺ (N4Py = *N,N'*-bis(2-pyridylmethyl)-*N*-bis(2-pyridyl)methylamine), [(TMC)Fe^{IV}(O)]²⁺ (TMC, 1,4,8,11-tetramethyl-1,4,8,11-tetraazacyclotetradecane) and [(TPFPP)Fe^{IV}(O)]²⁺ (TPFPP, *meso*-tetrakis(pentafluorophenyl)-porphyrinato dianion) complexes [29,30], where *N*-methylanilines were the exclusive reaction products without formation of *N*-methylformanilides. These

highly selective stoichiometric reactions can be proposed as a possible elementary step of the catalytic systems mentioned above.

We have recently been successful in obtaining well characterized synthetic analogues of high-valent non-heme iron species with N4Py-type pentadentate ligands, $[\text{Fe}^{\text{IV}}(\text{N4Py}^*)(\text{O})]^{2+}$ (**2**) ($\text{N4Py}^* = N,N\text{-bis}(2\text{-pyridylmethyl})\text{-}1,2\text{-di}(2\text{-pyridyl})\text{ethylamine}$), which have features in common with non-heme iron-dependent oxygenases [31] with respect to their structure and oxidative activity. These intermediates are shown to mediate a variety of monooxygenations, including aliphatic and aromatic hydroxylations [32,33], oxygenation of sulfides [31] and aldehydes [32], epoxidation of olefins [34], and Baeyer-Villiger oxidations [35]. Herein, we set out to explore the catalytic reactivity of the complex, $[(\text{N4Py}^*)\text{Fe}^{\text{II}}(\text{CH}_3\text{CN})](\text{ClO}_4)_2$ (**1**) towards *N,N*-dimethylanilines with TBHP, H_2O_2 , PAA and mCPBA as terminal oxidants, and wanted to get direct evidence for the formation of reactive intermediates, and their possible role in the oxidation (*N*-demethylation) process based on kinetic and spectroscopic studies (Fig.1).

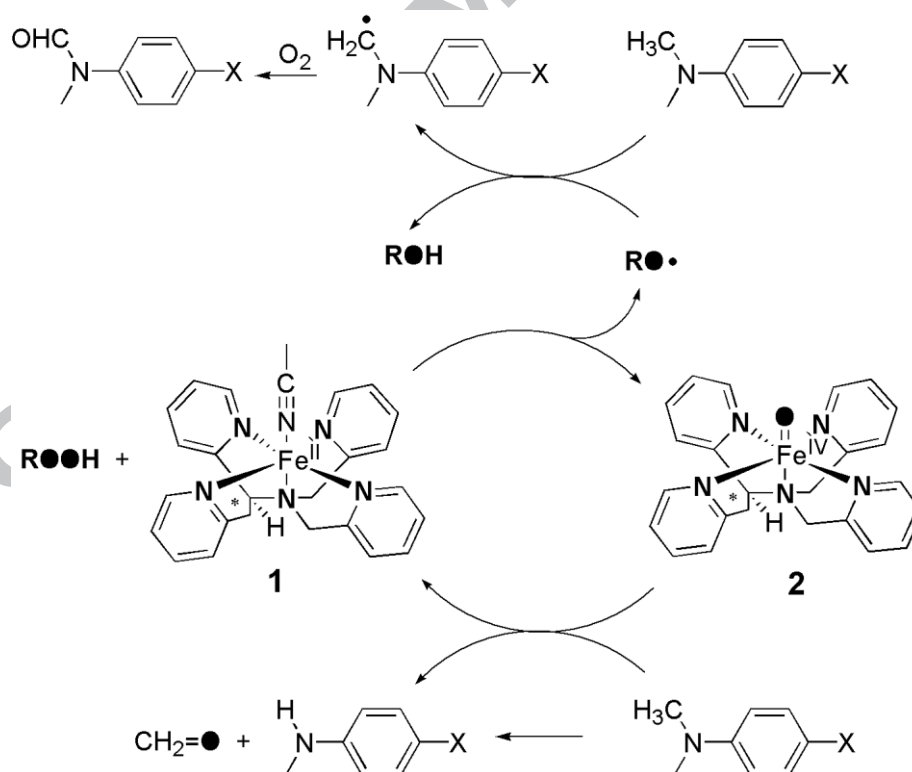


Fig. 1 Oxoiron(IV) mediated *N*-demethylation reaction in this study.

2. Experimental section

2.1. Materials and methods

The N_4Py^* ligand, and its $[Fe^{II}(N_4Py^*)(CH_3CN)](ClO_4)_2$ (**1**) complex were prepared according to published procedures [31]. UV/Vis spectra were recorded with an Agilent 8453 diode-array spectrophotometer with quartz cells. GC analyses were performed on Shimadzu QP2010SE equipped with a secondary electron multiplier detector with conversion dynode and a 30 m HP-5MS column.

2.2. Description of the catalytic oxidation reactions

In a typical reaction, 1 mL of H_2O_2 (diluted from 35% solution), mCPBA (77%), PAA (diluted from 38-40% solution) or TBHP (diluted from 70% solution) solution in CH_3CN was delivered by syringe pump in air (Ar) to a stirred solution (2 mL) of catalyst **1** or $Fe(ClO_4)_2$ salt, and DMA substrate inside a vial. The final concentrations were 3 mM catalyst **1**, 150 mM co-oxidant, and 300 mM substrate. The PhIO was added as a solid into the CH_3CN solution containing 100 μ L H_2O due to the poor solubility of PhIO. The products were identified by GC, GC/MS analysis, and their yields were determined by comparison with authentic compounds using bromobenzene as an internal standard in the reactions. The HCHO was identified as 2,4-dinitrophenylhydrazone by GC/MS ($M^+ = 210$).

2.3. Stoichiometric oxidation of *N,N*-dimethylaniline with $[Fe^{IV}(N_4Py^*)(O)]^{2+}$ (**2**)

All reactions were carried out under thermostated conditions at different temperature in 1 cm quartz cuvettes with stirring under argon. $[Fe^{II}(N_4Py^*)(CH_3CN)](ClO_4)_2$ complex (2.00×10^{-3} M) was dissolved in acetonitrile (1.5 mL), then iodosobenzene (3.00×10^{-3} M) was added to the solution. The mixture was stirred for 50 minutes then excess iodosobenzene was removed by filtration. The rate of substrate oxidation was followed by monitoring the decrease in absorbance at 705 nm ($\epsilon = 400 \text{ M}^{-1} \text{ cm}^{-1}$), under pseudo-first order condition of excess DMA derivatives.

3. Results and discussion

3.1. Catalytic oxidation of *N,N*-dimethylaniline (DMA) derivatives

As reported earlier, DMA can be oxidized by iron salts via one-electron oxidation to dimerized product (D) as the predominant product with small amount of demethylated *N*-methylaniline (D/MA = 1.7; TON = ~ 40 at 60°C after 10 h.) under molecular oxygen. In contrast, in the presence of iron-salen complexes the *N*-methylformanilide was the major product with MA (MFA/MA = ~2; TON = 180 at 60°C after 10 h.). Aminium cation radical

has been suggested for the former, and α -amino radical for the latter case as key species, but the iron-based intermediates are still unclear [24,25]. To get more insight into the mechanism of this curious reaction the catalytic activity and selectivity of $[\text{Fe}^{\text{II}}(\text{N4Py}^*)(\text{CH}_3\text{CN})]^{2+}$ (**1**), where the possible reactive high-valent intermediate ($\text{Fe}^{\text{IV}}\text{O}$) is known and spectroscopically well characterized, was studied in the oxidation of DMA derivatives, utilizing TBHP, H_2O_2 , PAA and mCPBA as co-oxidants compared to the corresponding $\text{Fe}^{\text{II}}(\text{ClO}_4)_2$ /co-oxidant system (Table 1). Reactions were carried out under standard catalytic conditions (1 : 100 : 50 for the catalyst : DMA : co-oxidant) in acetonitrile at room temperature under air (Ar). Co-oxidants were added by syringe, and the excess of DMA was used to minimize the over-oxidized products. The catalytic activity and selectivity of **1** and the iron(II) salt appeared to be dependent on the co-oxidants used for oxidation. The $\text{Fe}^{\text{II}}(\text{ClO}_4)_2$ salt together with H_2O_2 oxidizes DMA to MA and MFA, and a turnover number (TON) of 2.9 and 0.8 was obtained with an overall yield of 7.5% (the sum of both MA and MFA; based on co-oxidant), respectively. Almost identical result has been observed by the use of TBHP as co-oxidant (3.3 and 0.8 TON, respectively), with a similar MA to MFA ratio (3.7 vs. 4.4 for TBHP). When mCPBA and PAA were used as co-oxidants significantly higher activities were observed (TON of 10 vs. 16 with MA/MFA = 4.2 vs. 6.5 for PAA). The increased reactivity of peracids compared to H_2O_2 and TBHP may be explained by the in situ formed $[\text{Fe}_3\text{O}(\text{OAc})_3]^+$ and $[\text{Fe}_3\text{O}(\text{mCBA})_3]^+$ complexes with a remarkably higher catalytic activities compared to the parent $\text{Fe}(\text{ClO}_4)_2$ salt [25]. The catalytic activity of **1** was also examined including the same co-oxidants, and conditions used above, facilitating direct comparison with results obtained with the parent iron(II) salt. Table 1 and Fig. 2 show that there is an increase of the overall yield when the oxidants employed are PhIO, H_2O_2 , TBHP, mCPBA, and PAA (from 11 to 69%), albeit with moderate product selectivity, significantly lower MA/MFA ratios (2.2, 2 and 2.5 for H_2O_2 , TBHP and PAA, respectively) except of 1/mCPBA system (MA/MFA = 6). The result of PhIO-containing system was not included in Fig. 2 due to the observed inhomogeneity. The low MA/MFA ratio indicates an autooxidation process via Russel-type termination mechanism involving reaction of the $\text{PhC}(\text{Me})\text{CH}_2\cdot$ radical with dioxygen to form equimolar amount of $\text{PhC}(\text{Me})\text{CH}_2\text{OH}$ and $\text{PhC}(\text{Me})\text{CHO}$, and finally MA and CH_2O from the former hydroxy intermediate. The formation of $\text{PhC}(\text{Me})\text{CH}_2\cdot$ radical may be explained by the appearance of hydroxyl (*tert*-butoxy) radical during the formation of oxoiron(IV) species. In case of mCPBA and PhIO the presence of highly reactive hydroxyl radical can be excluded, but the formation of MFA could occur via reaction between cage-escaped $\text{PhC}(\text{Me})\text{CH}_2\cdot$ radical (derived from the reaction of **2** with DMA) and dioxygen. In summary,

it can be concluded that the moderate selectivity can be explained by the parallel selective metal-based, and non-selective radical processes resulting in MA and MFA-MA as main products, respectively. In the **1**/H₂O₂/DMA reaction system, 2,6-di-*tert*-butyl-4-methylphenol as a radical trap was used, and it was found that the reaction was inhibited by its presence (12 vs. 4 TON with significantly higher MA to MFA ratio MA/MFA = 2.2 vs. 4.1), suggesting that the oxidation of DMA catalyzed by **1** should really involve radical species, and the MFA derives from its reaction. Similar result has been observed for the anaerob **1**/PhIO/DMA system in the presence of radical trap. Further evidence for this assumption, that no formation of MFA occurred when the oxidation of DMA was carried out in the presence of **1** with PhIO, PAA, mCPBA and TBHP as co-oxidants under argon, whilst the MA was the exclusive product with 10.9, 29, 26.3 and 10.9 yields. In case of the H₂O₂ the presence of dioxygen can be explained by the metal-based disproportionation of H₂O₂. *Para*-substituted *N,N*-dimethylanilines were observed to produce corresponding secondary anilines where anilines with electron-donating groups on the phenyl ring gave better yields and selectivity than those with electron-withdrawing groups, suggesting a metal-based oxidant with electrophilic character (Fig. 3). It can also be seen that the product composition (MA/MFA ratio) being remarkably influenced by the electron density on the substrate (Fig. 4), especially in the **1**/mCPBA system.

Table 1

Iron-catalyzed oxidation of *N,N*-dimethylanilines with various co-oxidants under air^a and argon^b.

[1]:[DMA]:[Co-oxidant] ^a	Yield (%) ^c 4R-MA	TON ^{MA}	Yield (%) ^c 4R-MFA	TON ^{MFA}	MA/MFA	TON
1 ^c :100:50 (PAA) ^a	27.3 ^H	13.8	4.2 ^H	2.1	6.5	16
1 . 100 :50 (PAA) ^a	48.9 ^H	24.5	19.7 ^H	9.8	2.5	34
1 . 100 :50 (PAA) ^b	29 ^H	14.3	-	-		14
1 ^d :100:50 (mCPBA) ^a	17 ^H	8.5	3.9 ^H	1.8	4.2	10
1 . 100 :50 (mCPBA) ^a	43.9 ^{Me}	21.9	6.6 ^{Me}	3.3	6.7	25
1 . 100 :50 (mCPBA) ^a	36.9 ^H	18.5	6.2 ^H	3.1	6	22
1 . 100 :50 (mCPBA) ^b	26.3 ^H	13.2	-	-		13
1 . 100 :50 (mCPBA) ^a	31.6 ^{Br}	15.8	6.5 ^{Br}	3.2	4.9	19
1 . 100 :50 (mCPBA) ^a	23.2 ^{CN}	11.6	6.0 ^{CN}	3	3.9	15

1 ^d . 100 :50 (TBHP) ^a	6.6 ^H	3.3	1.5 ^H	0.8	4.4	4
1 . 100 :50 (TBHP) ^a	21.3 ^H	10.6	10.3 ^H	5.2	2.0	16
1 . 100 :50 (TBHP) ^b	10.9 ^H	5.5	1>	0.5>		6
1 ^d . 100 :50 (H ₂ O ₂) ^a	5.9 ^H	2.9	1.58 ^H	0.8	3.7	4
1 . 100 :50 (H ₂ O ₂) ^a	20.4 ^{Me}	10.2	7.4 ^{Me}	3.7	2.8	14
1 . 100 :50 (H ₂ O ₂) ^a	15.9 ^H	8	7.1 ^H	3.5	2.2	12
1 . 100 :50 (H ₂ O ₂) ^b	11.2 ^H	5.6	2.5 ^H	1.2	4.5	7
1 . 100 :50 (H ₂ O ₂) ^c	6.1 ^H	3.1	1.6 ^H	0.8	4.1	4
1 . 100 :50 (H ₂ O ₂) ^a	11.3 ^{Br}	5.6	8.0 ^{Br}	4	1.4	10
1 . 100 :50 (H ₂ O ₂) ^a	7.82 ^{CN}	3.9	8.3 ^{CN}	4.2	0.9	8
1 . 100 :50 (PhIO) ^a	10.9 ^H	5.4	1.0 ^H	0.5		4
1 . 100 :50 (PhIO) ^b	10.9 ^H	5.4	-	-	-	5
1 . 100 :50 (PhIO) ^{b,e}	0.6 ^H	0.3	-	-		0.3

^aReaction conditions: see Experimental section. ^cBased on oxidant. ^dFe(ClO₄)₂ was used as catalyst. ^eReaction in the presence of 2,6-di-*tert*-butyl-4-methylphenol (15 equiv.).

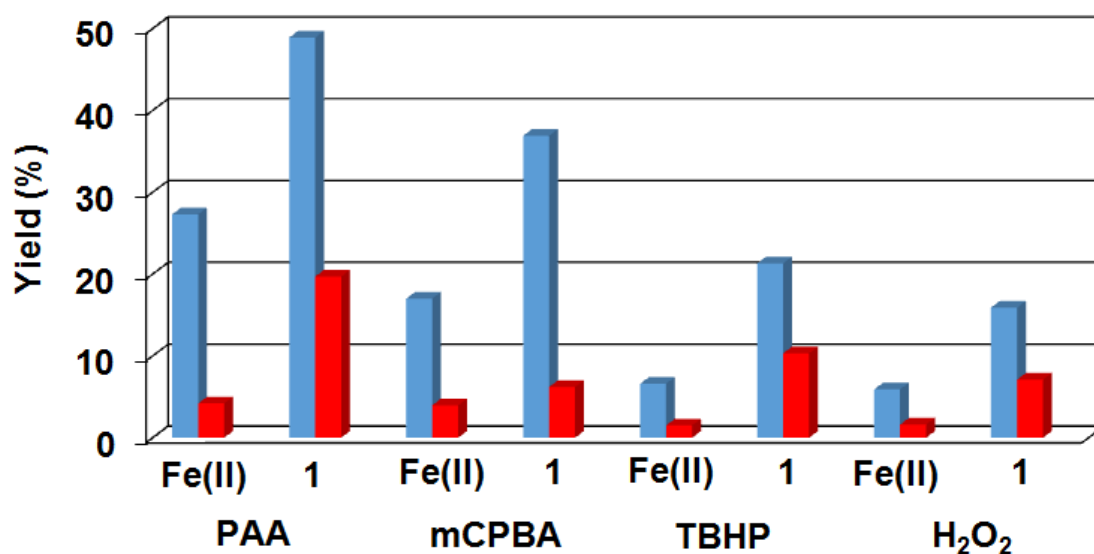
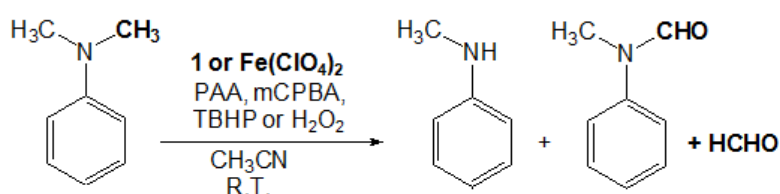


Fig. 2 Comparison of the product formation in the iron-catalyzed ($\text{Fe}(\text{ClO}_4)_2$ vs. **1**) oxidation of *N,N*-dimethylaniline to *N*-methylaniline (blue) and *N*-methylformanilide (red) with various co-oxidants in CH_3CN at 25°C under air.

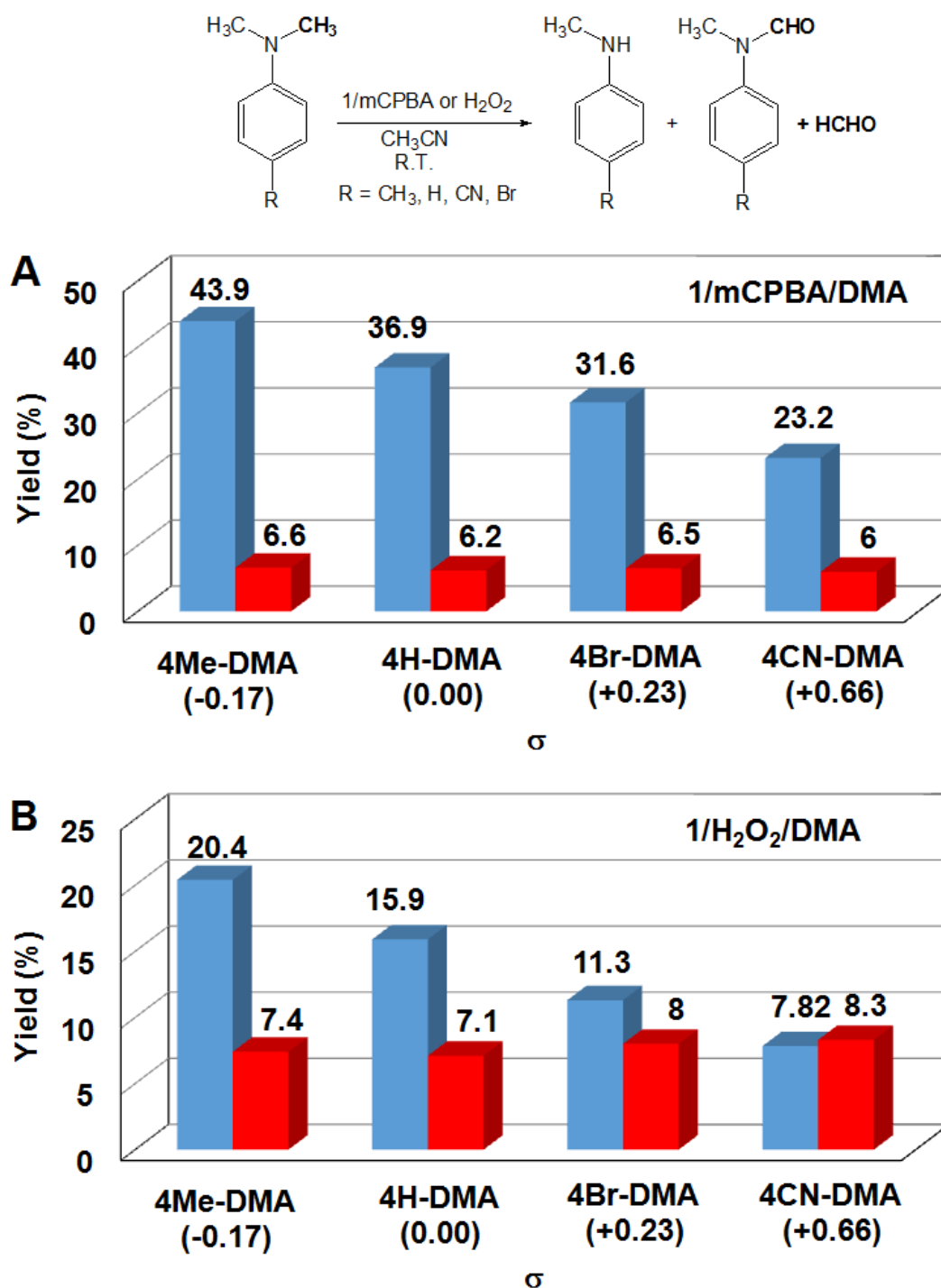


Fig. 3 Comparison of the product formation in the iron-catalyzed (**1**) oxidation of substituted *N,N*-dimethylanilines to *N*-methylaniline (blue) and *N*-methylformanilide (red) derivatives with mCPBA (**A**) and H_2O_2 (**B**) in CH_3CN at 25°C under air.

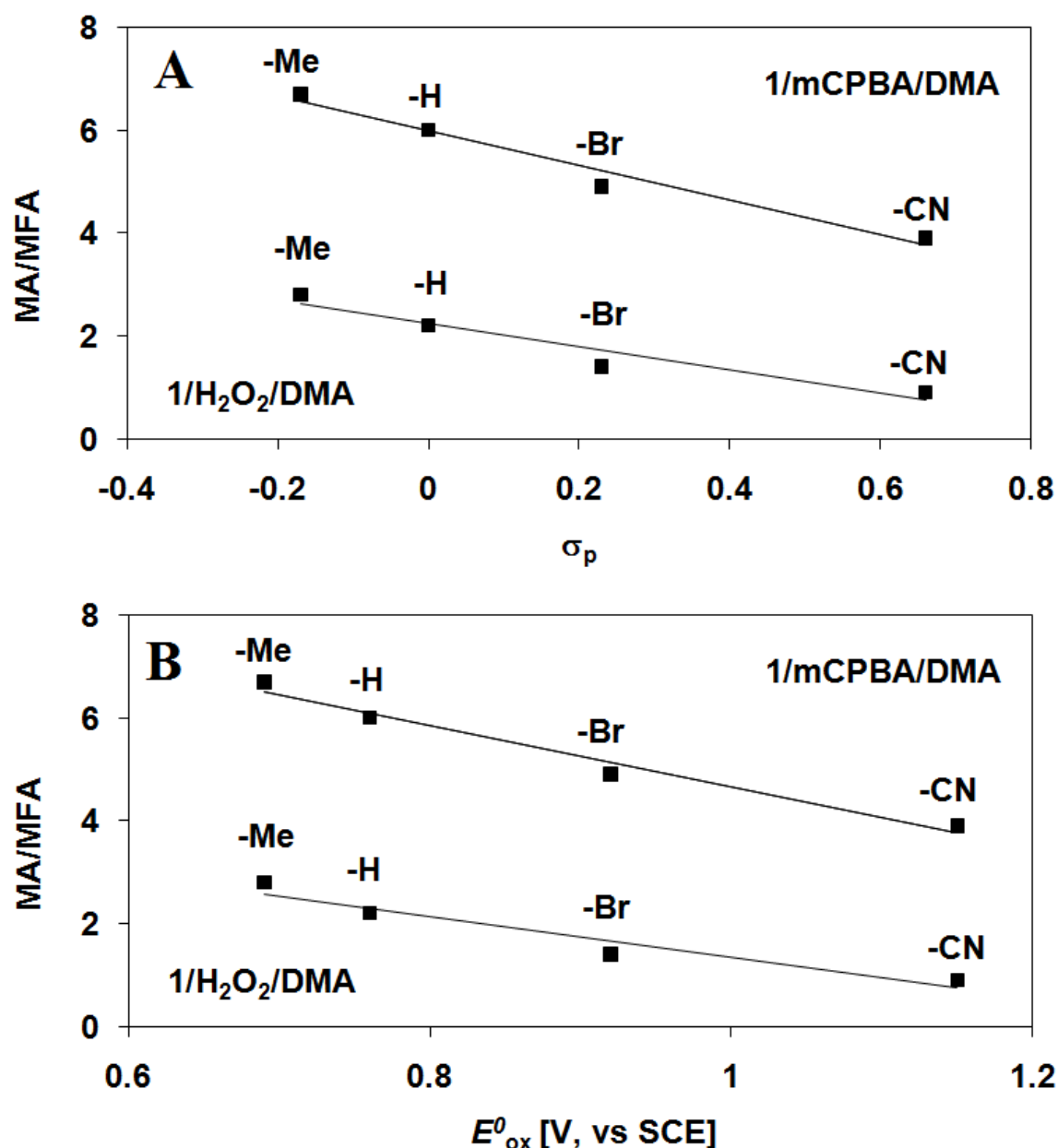


Fig. 4 Reactions of $[\text{Fe}^{\text{II}}(\text{N}_4\text{Py}^*)(\text{CH}_3\text{CN})](\text{ClO}_4)_2$ with DMAs by the use of mCPBA and H_2O_2 in CH_3CN at 25°C under air. (A) Plot of MA to MFA ratio against the σ_p of *para*-substituted DMAs. (B) Plot of MA to MFA ratio against the E^0_{ox} of *para*-substituted DMAs.

Anaerobic spectral investigations were also performed to trap the possible intermediates. The UV-Vis measurements in the absence of DMA using various co-oxidants (mCPBA, PAA, TBHP, and H_2O_2) have confirmed the formation of oxoiron(IV) species **2** (Fig. 5A) [31]. We have shown earlier that the complex **1** forms very stable high valent oxoiron(IV) species (**2**) with PhIO in CH_3CN ($t_{1/2} = 233$ h at R.T.; $\lambda_{\text{max}} = 705$ nm, $\varepsilon = 400 \text{ M}^{-1}\text{cm}^{-1}$) (Fig. 5A) [31]. Its

yield and the observed red shift on the λ_{max} values (from 703 to 730 nm) can be explained by the reaction and/or interaction (H-bridge) of the oxoiron(IV) with the oxidant (PAA, mCPBA, TBHP, H_2O_2) and/or the solvent (*tert*-BuOH, AcOH, H_2O ...) used during the generation. In case of the H_2O_2 , its reaction with **1** in CH_3CN resulted in the formation of a transient purple species with a characteristic absorbance maximum at λ_{max} 535 nm ($\epsilon = 630 \text{ M}^{-1} \text{ cm}^{-1}$). It has a half-life of about 3 min at 25°C . These values are identical with those reported for low-spin N4Py-type $[(\text{N}3\text{PyBim})\text{Fe}^{\text{III}}(\text{OOH})]^{2+}$ systems with one 1-methyl-2-benzimidazolyl arm [36]. Its decay resulted in the formation of **2** (Fig. 5B). These results may suggest that a high-valent oxoiron(IV) species is one of the possible intermediate which is responsible for the demethylation reaction of DMA. However, we have to expect the presence of free radicals such as $\text{HO}\cdot$, $\text{tBuO}\cdot$, and dioxygen which may compete with the metal-based oxidation.

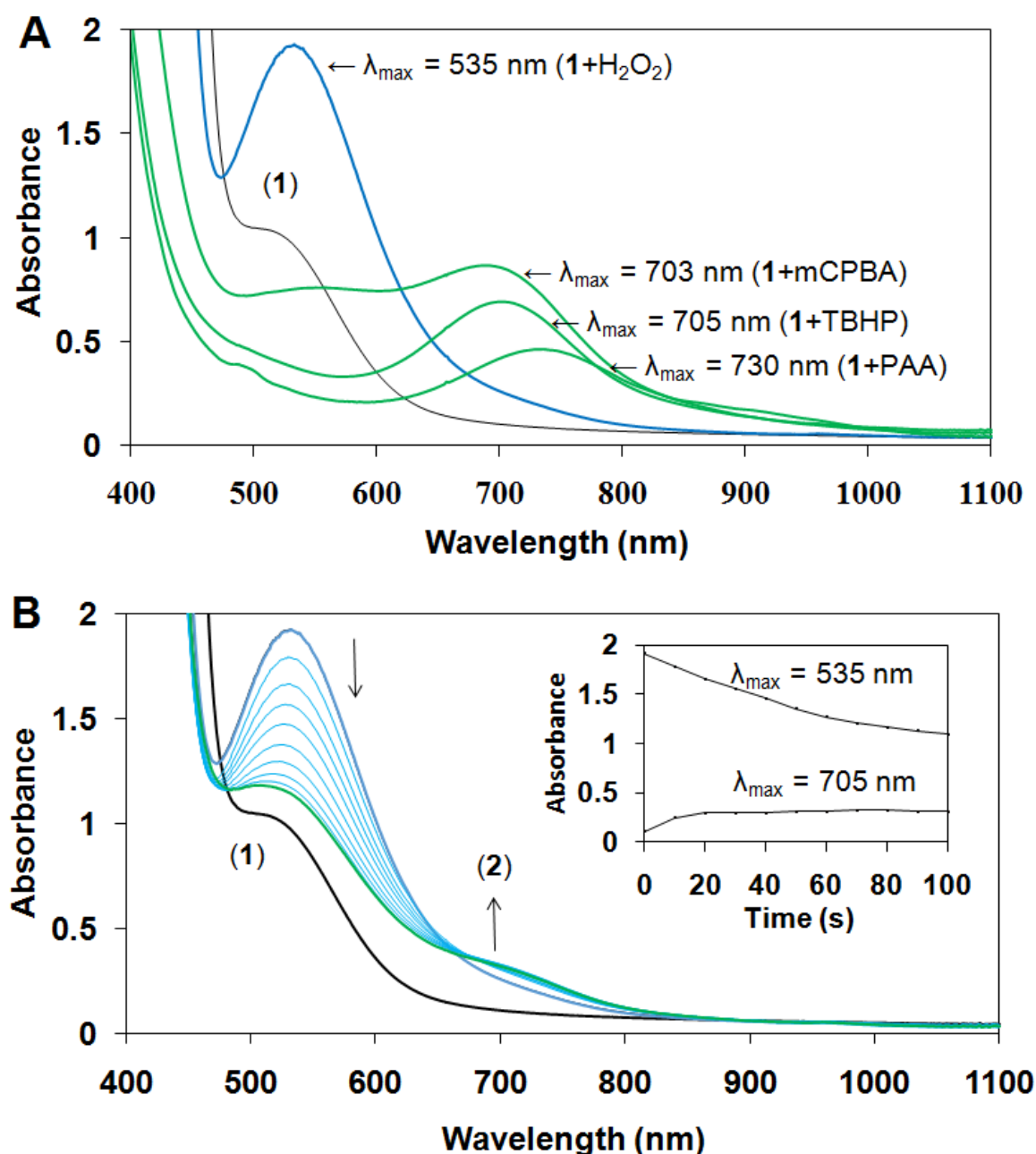


Fig. 5 The UV-Vis spectral change of **1** upon addition of various co-oxidants (PAA, mCPBA, TBHP and H₂O₂ at room temperature (A), and time courses of the decay of Fe^{III}OOH species derived from the reaction of **1** with H₂O₂, during the formation of **2**. [**1**] : [co-oxidant] = 1 : 50. ([**1**] = 3 mM) in CH₃CN at 25°C (B).

The UV-Vis experiments in the presence of DMA under the previously used standard catalytic conditions (1/H₂O₂/DMA = 1 : 50 : 100) have also confirmed the formation of oxoiron(IV) species **2**, that undergoes a decay, which is affected by the substrate, DMA (Fig. 6A). The shift in the λ_{\max} value of the oxoiron(IV) species in the presence of DMA from 705 to 750 nm, and the new intense absorption in the range of 5-600 nm indicates a complexation and charge-transfer (CT) type interaction between the oxidant and the substrate, albeit their

nature is not known. The same spectral changes can be observed when the substrate, DMA was added to the oxoiron(IV) species generated by the reaction of **1** and PhIO.

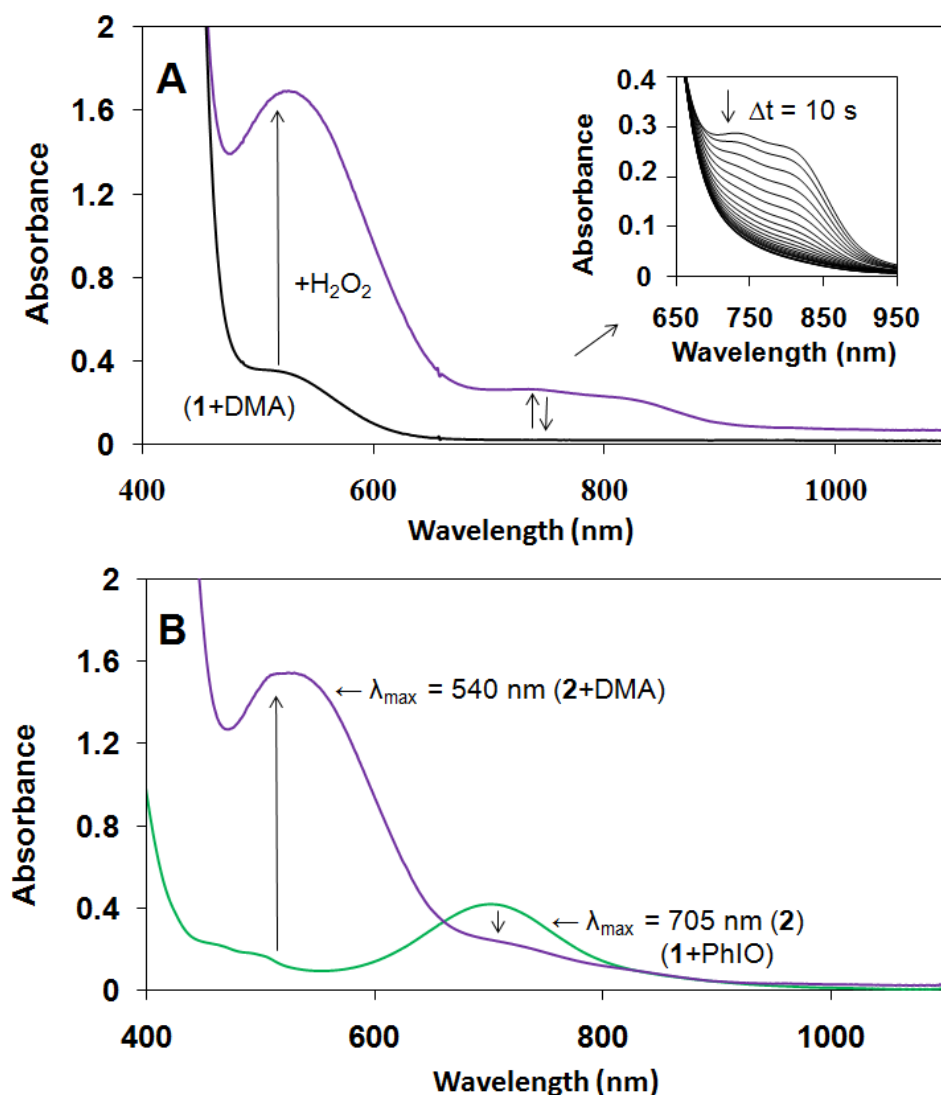


Fig. 6 The UV-Vis spectral changes of **1** and **2** (inset) species in the presence of DMA upon addition of H_2O_2 at room temperature, $[\mathbf{1}] : [\text{H}_2\text{O}_2] : [\text{DMA}] = 1 : 50 : 100$. ($[\mathbf{1}] = 3$ mM) in CH_3CN at 25°C (A), and the UV-Vis spectral change after addition of DMA to **2** (derived from the reaction of **1** with PhIO), $[\mathbf{2}] : [\text{DMA}] = 1 : 100$. ($[\mathbf{2}] = 3$ mM, $l = 0.5$ cm) in CH_3CN at 25°C (B).

3.1. Stoichiometric oxidation of *N,N*-dimethylaniline (DMA) derivatives with **2**

In the iron-catalyzed oxidation of DMA with terminal oxidants two processes can be proposed as rate-controlling step, namely the formation of high-valent oxoiron(IV) species from the reaction of precursor complex with the correspondent co-oxidant, or the reaction of oxometal species with the substrate. To avoid this difficulty, and to get more insight into the mechanism

of the *N*-demethylation process we have synthesized the oxoiron(IV) complex **2** by in situ reaction of **1** with PhIO, and investigated the stoichiometric oxidation of DMA with it. In this way, the formation of hydroxyl and *tert*-butoxy radicals and their non-selective reactions with the substrate in the stoichiometric reaction can be excluded, and the role of the oxoiron(IV) species can be directly investigated. Complex **2** is able to oxidize the *N,N*-dimethylanilines under mild anaerob conditions, at 15°C, in CH₃CN, and the GC and GC/MS analysis of the product indicated the formation of MA (yields ~80% based on **2**) as the main product with CH₂O. The kinetics of *N*-demethylation of DMAs with **2** were followed under pseudo-first-order conditions in the presence of 10-30-fold excess of substrate over the oxidant by measuring the change in the absorbance maximum at λ_{\max} 705 nm of **2** with time at 5-20°C. The reaction shows 1st-order dependence on both the oxoiron(IV) and the substrate concentration with $k_2 = (9.8 \pm 0.4) \times 10^{-2} \text{ M}^{-1} \text{ s}^{-1}$ (Fig. 7a), $\Delta H^\ddagger = 68 \text{ kJ mol}^{-1}$ and $\Delta S^\ddagger = -121 \text{ J mol}^{-1} \text{ K}$ for DMA (Table 2). Reaction rate obtained for the oxidation of DMA is smaller by one order of magnitude than those observed for oxoiron(IV) complexes with N4Py and TMC ligands ($k_2 = 1.4 \pm 0.1$ and $1.2 \pm 0.1 \text{ M}^{-1} \text{ s}^{-1}$, respectively [30]), but larger by two order of magnitude than that observed for Fe^{IV}O/TPFPP system ($(3.0 \pm 0.2) \times 10^{-4} \text{ M}^{-1} \text{ s}^{-1}$). The relatively large negative entropy is typical of associative processes (Fig. 7b). Based on previous catalytic results above, it can be expected that the *N*-demethylation reaction is sensitive to the nature of the substituent in the phenyl ring of DMAs. Upon using *para*-substituted DMA derivatives with electron donating groups the rate of the stoichiometric reactions were increased remarkably (Table 3, Fig. 7c). Based on the competitive reactions, the Hammett correlation ($r = 0.98$, $n = 5$, $\rho = -1.99$) demonstrates that the rate constant for the *N*-demethylation of DMA by **2** is much more sensitive to changes in the electronic properties of the DMA compared to the **2**/PhCH₂OH and **2**/PhCH₃ systems including rate-determining HAT process ($\rho = -0.32$, and $\rho = -0.98$, respectively) [38]. Furthermore this ρ value almost identical to that measured in the [Fe^{IV}(N4Py)(O)]²⁺/DMA system ($\rho = -2.1$), where electron transfer (ET) and concomitant proton transfer (PT) was proposed with a rate-determining PT step (Table 2 and 3) [29,30]. The correlation of log k_2 values with the one-electron oxidation potentials of DMAs (E°_{ox}) is good, and the slope (-4.1) is comparable to those obtained for the [Fe^{IV}(N4Py)(O)]²⁺/DMA (-3.3), [Fe^{IV}(TMC)(O)]²⁺/DMA (-4.0) and [Fe^{IV}(TPFPP)(O)]²⁺/DMA (-5.0) systems (Fig. 7d, Table 2 and 3). The magnitude of these values is also in a good agreement with the previously suggested ET-PT mechanism.

Table 2

Kinetic parameters determined in the oxidation of *N,N*-dimethylanilines by oxoiron(IV) complexes in acetonitrile at 25°C.

$[(L)Fe^{IV}(O)]$ L	k_2 ($M^{-1}s^{-1}$)	ρ	slope ($\log k_2$ vs. E°_{ox})	ΔH^\ddagger ($kJmol^{-1}$)	ΔS^\ddagger ($Jmol^{-1}K^{-1}$)	ΔG^\ddagger ($kJmol^{-1}$)	Refs.
N4Py	1.4 ± 0.1	-2.2	-3.3				[30]
TMC	1.2 ± 0.1	-2.6	-4.0				[30]
TPFPP	$(3.0 \pm 0.2) \times 10^{-4}$	-3.3	-5.0				[30]
N4Py*	$(9.8 \pm 0.4) \times 10^{-2}$	-1.99	-4.1	68	-121	103	t. w.

Table 3

Kinetic parameters determined in the oxidation of *p*-X-*N,N*-dimethylanilines by $[Fe^{IV}(N4Py^*)(O)]^{2+}$ (**2**) in acetonitrile at 10°C.

X	σ_p	E°_{ox} (vs SCE, V) ^a	k_2 ($M^{-1}s^{-1}$)
NMe ₂	-0.83	n.a.	$(14.5 \pm 0.5) \times 10^{-1}$
Me	-0.17	0.69	$(9.21 \pm 0.3) \times 10^{-2}$
H	0	0.76	$(7.45 \pm 0.1) \times 10^{-2}$
Br	0.23	0.92	$(1.95 \pm 0.04) \times 10^{-2}$
CN	0.66	1.15	$(1.35 \pm 0.04) \times 10^{-3}$

^aData from [37]

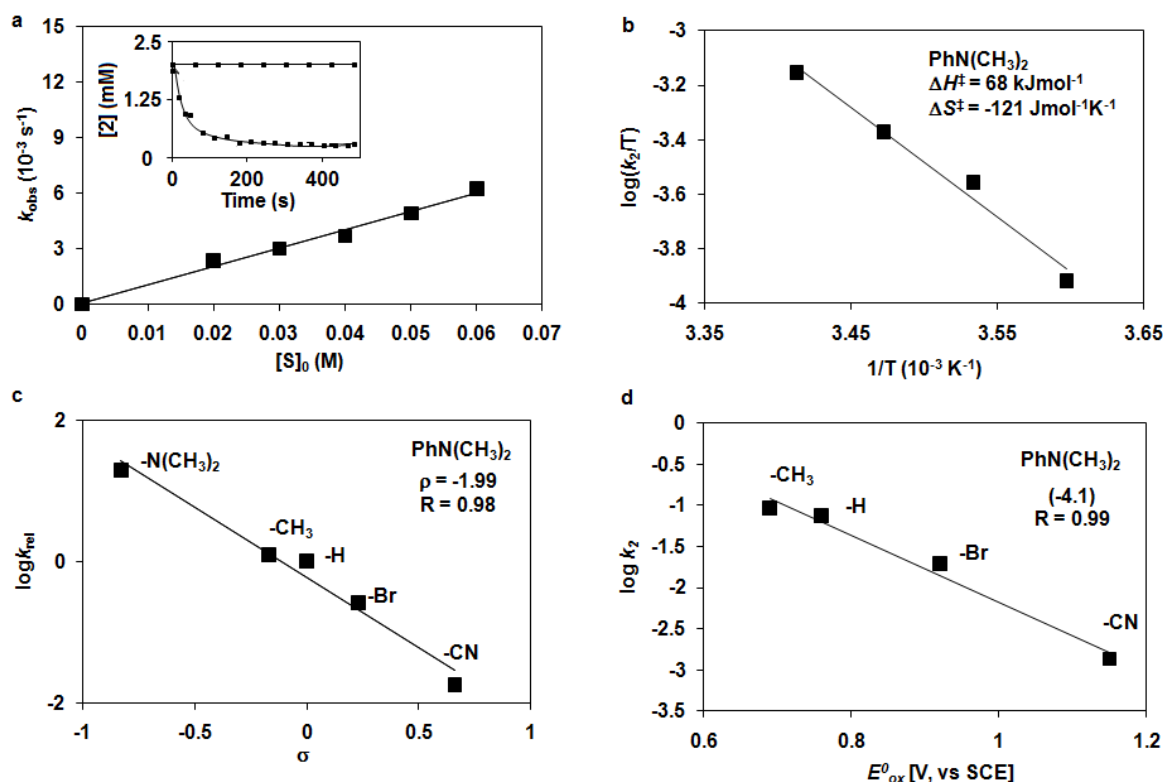


Fig. 7 Reactions of $[\text{Fe}^{\text{IV}}(\text{N4Py}^*)(\text{O})]$ (**2**) with DMAs in CH_3CN . (a) Plot of k_{obs} versus [substrate] for reactions of **2** (2mM) with DMA at 288 K. Inset shows time course of the decay of **2** monitored at 705 nm with DMA ($[\text{2}]_0 = 2 \text{ mM}$, $[\text{DMA}]_0 = 40 \text{ mM}$). (b) Eyring plot of $\log k_2/T$ versus $1/T$ for DMA ($[\text{2}]_0 = 2 \text{ mM}$, $[\text{DMA}]_0 = 40 \text{ mM}$). (c) Hammett plot of $\log k_{\text{rel}}$ against the σ_p of *para*-substituted DMAs. (d) Plot of $\log k_2$ against the E^0_{ox} of *para*-substituted DMAs.

4. Summary and conclusions

Efforts have been made to work out a highly efficient and highly selective iron(II)-catalyzed *N*-demethylation reactions by the use of various co-oxidants such as PhIO, mCPBA, PAA, TBHP and H_2O_2 , as well as their detailed mechanistic aspects. As a catalyst the $[(\text{N4Py}^*)\text{Fe}^{\text{II}}(\text{CH}_3\text{CN})](\text{ClO}_4)_2$ complex was chosen, where the possible reactive high-valent intermediate ($\text{Fe}^{\text{IV}}\text{O}$) is known and spectroscopically well characterized. The order of efficacy for the co-oxidants was found to be $\text{PAA} > \text{mCPBA} > \text{TBHP} > \text{H}_2\text{O}_2 > (\text{PhIO})$ in the presence of the iron(II) catalyst, which can be explained by the different mechanism of the oxoiron(IV) formation and the presence/absence of hydroxyl (*tert*-butoxy) radicals. In case of PAA, mCPBA and PhIO the reaction proceeds via oxene transfer, where the stoichiometry of $\text{Fe}^{\text{II}}/\text{oxidant} = 1$, whilst with H_2O_2 and TBHP via Fe^{III} -intermediates ($\text{Fe}^{\text{II}}/\text{oxidant} = 1.5$),

resulting hydroxyl (*tert*-butoxy) radicals. It was also found that the selectivity, the product composition (MA/MFA) remarkably depends on the electron density on the substrate and the nature of the co-oxidants used. The highest selectivities have been found for mCPBA (MA/MFA = ~6) and PhIO, where no formation of MFA occurred during the oxidation. To get a plausible mechanism for the catalytic reaction, the capture and characterization of the possible intermediates, and their test against the substrate are the most important tasks. Based on spectroscopic and kinetic investigations on the **1**/co-oxidant/DMA systems we have found a direct and convincing proof for the formation of high-valent oxoiron(IV) species in all cases and for its key role in the catalytic cycle. Based on experimental observations derived from the catalytic and stoichiometric experiments the following mechanisms can be proposed (Fig. 8). In the peracid and PhIO-based systems the formation of oxoiron(IV) can be explained by direct oxygen atom transfer from the co-oxidant to the Fe(II) precursor: $\text{Fe}^{\text{II}} + \text{PhIO (mCPBA)} = \text{Fe}^{\text{IV}}\text{O} + \text{PhI (mCBA)}$, while in the H_2O_2 -based system as a result of the decomposition of the transient $[\text{Fe}^{\text{III}}(\text{OOH})]^{2+}$ species: $[\text{Fe}^{\text{III}}(\text{OOH})]^{2+} \rightarrow \text{Fe}^{\text{IV}}\text{O} + \text{HO}\cdot (\text{tBu}\cdot)$. In the former, clearly metal-based process only the oxoiron(IV) is responsible for the *N*-methylation reaction via ET-PT mechanism with a rate determining PT step (Path a in Fig. 8) [29], but in the latter case the reaction can be explained by the parallel selective metal-based and non-selective radical processes (Path a + b in Fig. 8) [39,40].

Fig. 8. Proposed mechanism in the iron(II)-catalyzed *N*-demethylation reaction.

Financial support of the Hungarian National Research Fund (OTKA K108489), and GINOP-2.3.2-15-2016-00049 are gratefully acknowledged.

- [1] F. P. Guengerich, J. Biol. Chem. 266 (1991) 10019.
- [2] F. P. Guengerich, L. T. Macdonald, Acc. Chem. Res. 17 (1984) 9.
- [3] T. D. Porter, M. J. Coon, J. Biol. Chem. 266 (1991) 13469.
- [4] P. F. Hollenberg, FASEB J. 6 (1992) 686.
- [5] R. P. Hanzlik, K.-H. J. Ling, J. Am. Chem. Soc. 115 (1993) 9363.
- [6] M. Newcomb, R. Shen, S.-Y. Choi, P. H. Toy, P. F. Hollenberg, A. D. Vaz, M. J. Coon, J. Am. Chem. Soc. 122 (2000) 2677.
- [7] P. H. Toy, M. Newcomb, P. F. Hollenberg, J. Am. Chem. Soc. 120 (1998) 7719.

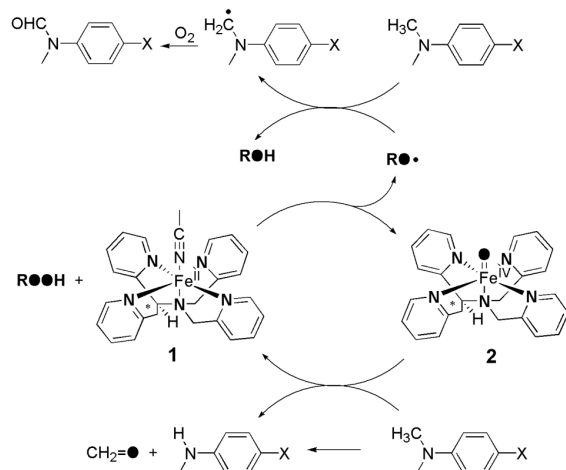
- [8] X.-X. Li, Y. Wang, Q.-C. Zheng, H.-X. Zhang, *J. Inorg. Biochem.* 154 (2016) 21.
- [9] L. T. Macdonald, K. Zirvi, L. T. Burka, P. Peyman, F. P. Guengerich, *J. Am. Chem. Soc.* 104 (1982) 2050.
- [10] R. A. Stearns, P. R. Ortiz de Montillano, *J. Am. Chem. Soc.* 107 (1985) 4081.
- [11] O. Augusto, H. S. Beilan, P. R. Ortiz de Montillano, *J. Biol. Chem.* 257 (1982) 11288.
- [12] T. Shono, T. Toda, N. Oshino, *J. Am. Chem. Soc.* 104 (1982) 2639.
- [13] G. T. Miwa, J. S. Walsh, G. L. Kedderis, P. F. Hollenberg, *J. Biol. Chem.* 265 (1990) 12349.
- [14] P. F. Guengerich, C.-H. Yun, T. L. Macdonald, *J. Biol. Chem.* 271 (1996) 27321.
- [15] S. B. Karki, J. P. Dinnocenzo, J. P. Jones, K. R. Korzekwa, *J. Am. Chem. Soc.* 117 (1995) 3657.
- [16] J. I. Manchester, J. P. Dinnocenzo, L. A. Higgins, J. P. Jones, *J. Am. Chem. Soc.* 119 (1997) 5069.
- [17] B. W. Griffin, P. L. Ting, *Biochemistry* 17 (1978) 2206.
- [18] J. Van der Zee, R. Duling, R. P. Mason, T. E. Eling, *J. Biol. Chem.* 264 (1989) 19828.
- [19] G. T. Miwa, J. S. Walsh, G. L. Kedderis, P. F. Hollenberg, *J. Biol. Chem.* 258 (1983) 14445.
- [20] J. R. Lindsay Smith and D. N. Mortimer, *J. Chem. Soc., Chem. Commun.* (1985) 64.
- [21] C. Yi, C. He, *Acc. Chem. Res.* 42 (2009) 519.
- [22] J. M. Hagel, P. J. Facchini, *Front. Physiol.* 1 (2010) 1.
- [23] J. R. Lindsay Smith and D. N. Mortimer, *J. Chem. Soc., Perkin Trans. 2* (1986) 1743.
- [24] S. Murata, M. Miura, M. Nomura, *J. Org. Chem.* 54 (1989) 4700.
- [25] S. Murata, M. Miura, M. Nomura, *J. Chem. Soc., Chem. Commun.* (1989) 116.
- [26] D. Narog, U. Lechowicz, T. Pietryga, A. Sobkowiak, *J. Mol. Catal. A. Chem.* 212 (2004) 25.
- [27] O. Meth-Cohn, S. P. Stanforth, *Compr. Org. Synth.* 2 (1991) 777.
- [28] A. Schall, O. Reiser, *Sci. of Synth.* 25 (2007) 609.
- [29] A. Barbieri, M. De Gennaro, S. Di Stefano, O. Lanzalunga, A. Lapi, M. Mazzonna, G. Olivoa, B. Ticconia, *Chem. Commun.*, 51 (2015) 5032.
- [30] K. Nehru, M. S. Seo, J. Kim, W. Nam, *Inorg. Chem.* 46 (2007) 293.
- [31] D. Lakk-Bogáth, R. Csonka, G. Speier, M. Reglier, A. J. Simaan, J. V. Naubron, M. Giorgi, K. Lazar, J. Kaizer, *Inorg. Chem.* 55 (2016) 10090.
- [32] R. Turcas, D. Lakk-Bogáth, G. Speier, J. Kaizer, *Dalton. Trans.* 47 (2018) 3248.

- [33] R. Turcas, B. Kripli, A.A.A. Attia, D. Lakk-Bogáth, G. Speier, M. Giorgi, R. Silaghi-Dumitrescu, J. Kaizer, Dalton. Trans. 47 (2018) 14416.
- [34] B.I. Meena, D. Lakk-Bogáth, B. Kripli, G. Speier, J. Kaier, Polyhedron 151 (2018) 141.
- [35] R. Turcas, D. Lakk-Bogáth, G. Speier, J. Kaizer, Inorg. Chem. Commun. 92 (2018) 141.
- [36] M. Mitra, H. Nimir, S. Demeshko, S.S. Bhat, S.O. Malinkin, M. Haukka, J. Lloret-Fillol, G.C. Lisensky, F. Meyer, A.A. Shteinman, W.R. Browne, D.A. Hrovat, M.G. Richmond, M. Costas and E. Nordlander, Inorg. Chem. 54 (2015) 7152.
- [37] S. Fukuzumi, K. Shimoosako, T. Suenobu, Y. Watanabe, J. Am. Chem. Soc. 125 (2003) 9074.
- [38] D. Lakk-Bogáth, B. Kripli, B.I. Meena, G. Speier, J. Kaizer, Inorg. Chem. Comm. 104 (2019) 165.
- [39] G.A. Russel, J. Am. Chem. Soc. 79 (1957) 3871.
- [40] P.A. MacFaul, D.D.M. Wayner, K.U. Ingold, Acc. Chem. Res. 31 (1998) 159.

Catalytic and stoichiometric oxidation of *N,N*-dimethylanilines mediated by nonheme oxoiron(IV) complex with tetrapyrridyl ligand

Dóra Lakk-Bogáth, Balázs Kripli, Bashdar I. Meena, Gábor Speier and József Kaizer*

Catalytic activity and selectivity of $[\text{Fe}^{\text{II}}(\text{N4Py}^*)(\text{CH}_3\text{CN})]^{2+}$, where the possible reactive high-valent intermediate ($\text{Fe}^{\text{IV}}\text{O}$) is known and spectroscopically well characterized, was studied in the oxidation of DMA derivatives, utilizing PhIO, TBHP, H_2O_2 , PAA and mCPBA as co-oxidants.



*Corresponding author. Tel.: +36 88 62 4720; Fax: + 36 88 62 4469.
E-mail address: kaizer@almos.uni-pannon.hu.